JAST (Journal of Animal Science and Technology) TITLE PAGE

Upload this completed form to website with submission

ARTICLE INFORMATION	Fill in information in each box below
Article Type	Research article
Article Title (within 20 words without abbreviations)	Rabbit meat extract alleviates diet-induced obesity with upregulation of browning-related markers and identification of a bioactive peptide
Running Title (within 10 words)	Rabbit meat extract modulates adipocyte metabolism
Author	In-Seon Bae1, Won-Seo Park1, Sang-Yeob Lee2, Jun-Sang Ham1
Affiliation	1 Animal Resources Food Tech Division, National Institute of Animal Science, RDA, Wanju 55365, Republic of Korea 2 Animal Welfare Division, National Institute of Animal Science, RDA, Wanju 55365, Republic of Korea
ORCID (for more information, please visit https://orcid.org)	In-Seon Bae (https://orcid.org/0000-0003-3543-8785) Won-Seo Park (https://orcid.org/0000-0003-2229-3169) Sang-Yeob Lee (https://orcid.org/0000-0001-8024-1135) Jun-Sang Ham (https://orcid.org/0000-0003-4966-6631)
Competing interests	No potential conflict of interest relevant to this article was reported.
Funding sources State funding sources (grants, funding sources, equipment, and supplies). Include name and number of grant if available.	This research was supported by the Cooperative Research Program for Agriculture Science and Technology Development (Project No. RS-2022-RD010371), Rural Development Administration, Korea.
Acknowledgements	This research work was carried out with the support of "Cooperative Research Program for Agriculture Science and Technology Development (Project No. RS-2022-RD010371)" Rural Development Administration, Korea.
Availability of data and material	Upon reasonable request, the datasets of this study can be available from the corresponding author.
Authors' contributions Please specify the authors' role using this form.	Conceptualization: Bae IS. Data curation: Park WS, Ham JS. Formal analysis: Lee SY. Methodology: Bae IS, Park WS. Software: Park WS. Validation: Ham JS. Investigation: Bae IS. Writing - original draft: Bae IS, Lee SY. Writing - review & editing: Bae IS, Park WS, Lee SY, Ham JS.
Ethics approval and consent to participate	The animal study was approved by the Institutional Animal Care and Use Committee (IACUC) of the National Institute of Animal Science (approval number: NIAS-2023-0614).
Declaration of generative AI	No AI tools were used in this article.

4 **CORRESPONDING AUTHOR CONTACT INFORMATION**

For the corresponding author (responsible for correspondence, proofreading, and reprints)	Fill in information in each box below
First name, middle initial, last name	In-Seon Bae
Email address – this is where your proofs will be sent	Isbae746@korea.kr
Secondary Email address	Isbae746@gmail.com
Address	1500, Kongjwipatjwi-ro, Iseo-myeon, Wanju-gun, Jeonbuk State
Cell phone number	+82-10-6325-0818
Office phone number	+82-063-238-7356
Fax number	+82-063-238-7397

5
6

Abstract

Metabolic disorders are primarily driven by the pathological buildup of adipose tissue resulting from a sustained caloric surplus. Although rabbit meat is considered a nutritionally valuable protein source, its potential role in metabolic regulation has not been fully characterized. The present research focused on investigating the anti-obesity properties of rabbit meat extract (RME) and determining its bioactive peptides. To this end, male mice received a high-fat diet (HF) for a 15-week period, with RME administered orally at 150 or 300 mg/kg dosages. We subsequently analyzed body weight fluctuations, fat tissue histology, and liver lipid deposition to monitor metabolic shifts. RME supplementation markedly reduced HF-induced body weight gain, adipocyte hypertrophy, and hepatic lipid deposition. These effects were associated with downregulation of adipogenic regulators (C/EBPα, PPARγ, and aP2) and upregulation of thermogenesis-related markers (UCP1, PGC1α, and PRDM16) in adipose tissue. To elucidate the molecular pathways involved, RME-derived peptides were identified via LC–MS/MS analysis, leading to the selection of five functional candidates. Of these, peptide-3(GEAGPQGARG) exhibited the most potent bioactivity, characterized by the upregulation of thermogenic genes and the concurrent downregulation of adipogenic markers within adipocytes. Notably, in adipocytes, the regulatory effects of GEAGPQGARG on AMPK–ACC signaling and thermogenesis-related markers were attenuated by Compound C, suggesting that AMPK-associated signaling may partly contribute to the metabolic activity of this peptide.

Keywords：Rabbit meat extract, obesity, adipose browning, bioactive peptide, adipogenesis

Introduction

Dysregulation of energy balance leading to excessive adipose tissue expansion is a central feature of obesity and contributes to metabolic dysfunction. Excessive expansion of adipose tissue serves as a primary driver of disrupted metabolic homeostasis, significantly elevating the susceptibility to obesity-linked pathologies, including non-alcoholic fatty liver disease, cardiovascular ailments, and type 2 diabetes [1,2]. Although the etiology of obesity is multifactorial, sustained caloric excess combined with reduced physical activity has been identified as a major driving force behind its increasing prevalence. Despite extensive research, effective strategies for preventing and managing obesity through dietary approaches remain an ongoing challenge, highlighting the need for the identification of novel functional food resources with metabolic regulatory potential [3,4].

Increasing evidence suggests that the transformation of white adipose tissue into thermogenically active adipocytes represents a promising approach for improving metabolic balance. Unlike white adipose tissue, which primarily stores energy, brown and beige adipocytes are specialized for thermogenesis. This process is largely mediated by uncoupling protein 1 (UCP1), a protein that promotes energy dissipation within the mitochondria. Such thermogenic activity enhances overall energy expenditure, positioning it as a promising therapeutic strategy for tackling obesity [5–8]. The regulation of these thermogenic events involves intricate intracellular signaling networks. Central to this coordination is AMP-activated protein kinase (AMPK), which serves as a master regulator of metabolic adaptation during periods of energy disparity [9]. AMPK activation has been shown to inhibit adipocyte differentiation while facilitating adipose browning and mitochondrial biogenesis [10,11].

Peptides generated from dietary proteins have been increasingly recognized as modulators of metabolic processes, with reported effects on lipid metabolism, energy balance, and adipocyte function [12–17]. A number of these peptides have been demonstrated to influence adipogenesis, lipid metabolism, and energy expenditure [18-20]. However, existing research has predominantly focused on plant-derived bioactive compounds [21-23], whereas the metabolic regulatory roles of animal-derived peptides, particularly those with clearly defined mechanisms, require further characterization.

In contemporary nutrition, rabbit meat has attracted attention as a nutritionally valuable livestock product owing to its high-quality protein content and favorable lipid profile [24,25]. Compared with conventional red meats, rabbit meat generally contains lower levels of fat and cholesterol and provides essential micronutrients and vitamins [26,27]. In addition, its polyunsaturated fatty acid composition, including omega-3 and omega-6 fatty acids, may contribute to its nutritional value [28,29]. From a functional food perspective, this protein-rich matrix may serve as a source of bioactive peptides generated during thermal extraction and/or enzymatic hydrolysis. However, unlike peptides derived from milk, fish, collagen, and other commonly studied protein sources, rabbit meat-derived peptides have rarely been investigated for their roles in adipocyte metabolism. In particular, it remains unclear whether RME contains peptide sequences capable of modulating adipogenesis, adipose browning-related marker expression, and AMPK-associated signaling. Therefore, defining the peptide components of RME and evaluating their metabolic activity may provide new insight into the use of rabbit meat as an animal-derived functional food resource. The objective of the present study was to assess the anti-obesity potential of RME using a high-fat diet-induced model, while evaluating its effects on browning-related marker expression and the regulation of adipogenesis. Furthermore, we characterized specific bioactive peptides within RME to determine their functional contributions to adipocyte metabolism, specifically focusing on the involvement of AMPK-dependent signaling cascades.

Materials and Methods

Preparation and characterization of rabbit meat extract (RME)

Rabbit meat used in this study was purchased from the Korea Rabbit and Deer Agricultural Cooperative, a commercial rabbit meat supplier in South Korea. The meat was obtained as commercially processed edible rabbit meat. Before extraction, visible fat, fascia, and connective tissues were manually removed to minimize variation derived from non-muscle tissues. Because the raw material was purchased as commercially processed meat, detailed information on breed, sex, age, carcass weight, rearing environment, and post-mortem aging conditions was not available. To produce the RME, 2 kg of the processed meat was combined with 2 L of distilled water in a non-woven pouch. This mixture was

subjected to thermal extraction for 12 h at 120 °C under a stabilized pressure of 30 psi. Once the heating process was complete, the fluid was recovered by mechanical compression of the bag. The extract then underwent centrifugation (3000 × g, 10 min, room temperature) to separate phases. We subsequently filtered the resulting supernatant to remove residual particulates, followed by lyophilization. The final powder was kept at −80 °C for subsequent analyses. This extraction condition was selected to reflect a conventional high-temperature, pressurized hot-water extraction process used for preparing meat-based extract or decoction-type food products. The extraction yield of lyophilized RME was calculated as the percentage of dried extract weight relative to the initial weight of raw rabbit meat used for extraction. Total protein content was determined using a Bradford protein assay with bovine serum albumin as the standard and expressed as mg protein/g dry weight of RME.

Animals and diets

The animal study protocols received ethical clearance from the National Institute of Animal Science's Institutional Animal Care and Use Committee (Approval No. NIAS-2023-0614). We housed six-week-old male C57BL/6J mice in a regulated environment, maintaining a temperature of 22 ± 3 °C and a humidity level of 55 ± 10% under a 12-hour light/dark photoperiod. All mice had ad libitum access to water and their respective diets. Following a one-week acclimation phase, the subjects were randomized into four cohorts (n = 8 each): a normal chow-fed control group, a high-fat diet (HF) group, and two HF groups receiving oral RME at either 150 mg/kg (HF + RME150) or 300 mg/kg (HF + RME300). This dietary regimen was sustained for 15 weeks, with the HF consisting of 60% fat-derived calories (D12492; Research Diets, Inc.). The doses of RME, 150 and 300 mg/kg body weight, were selected based on preliminary screening to evaluate low- and high-dose effects within a practical range for food-derived extracts in diet-induced obesity models. RME was delivered daily at 10:00 AM via oral gavage. Throughout the duration of the study, both caloric intake and body mass were recorded on a weekly basis.

Blood parameter analysis

To collect blood samples, cardiac puncture was performed on mice following a 12-hour fast. Serum was isolated by centrifuging the collected blood at 13,000 × g for 15 min at 4 °C and subsequently kept at −70 °C. For the biochemical profiling, we measured serum triglycerides, total cholesterol, and HDL cholesterol using diagnostic reagents from Asan Pharmaceutical Co., Ltd. (Seoul, Korea), with all procedures conducted according to the manufacturer's instructions. LDL cholesterol levels were determined through the Friedewald equation. Furthermore, serum AST and ALT enzymatic activities were quantified using analytical kits sourced from Abcam (Waltham, MA, USA).

Histological analysis

For histological examination, liver and epididymal white adipose tissue (eWAT) samples were fixed for 24 h in a 10% neutral buffered formalin solution. Following fixation, the specimens were embedded in paraffin blocks and sliced into 5-μm-thick sections. General morphological features were visualized through hematoxylin and eosin (H&E; Abcam) staining. Images of the tissue architecture were recorded using the Optiview imaging system (Korea Lab Tech, Seongnam, Korea). To assess adipocyte hypertrophy, we quantified the cross-sectional areas of at least 50 individual adipocytes per sample using ImageJ software (National Institutes of Health, USA).

Western blot analysis

To extract total protein, adipose tissue samples were disrupted using RIPA lysis buffer (Sigma-Aldrich, St. Louis, MO, USA) supplemented with protease and phosphatase inhibitor cocktails. After a 20-minute incubation on ice, the homogenates were clarified by centrifugation at 14,000 × g for 15 min at 4 °C. We quantified protein concentrations using the Bradford method. Equal amounts of protein were resolved via 10–12% SDS-PAGE and then transferred onto nitrocellulose membranes. Non-specific sites were blocked using 5% skim milk for 1 h at room temperature. The membranes were then probed overnight at 4 °C with primary antibodies against AMPK and p-AMPK (Cell Signaling Technology, Danvers, MA, USA), as well as UCP1, PGC1α, PRDM16, PPARγ, C/EBPα, and aP2 (Abcam). Following TBST washes, secondary antibodies conjugated with horseradish peroxidase were applied. Immunoreactive bands were

detected through enhanced chemiluminescence (ECL) and their intensities were measured with iBright analysis software (ver. 5.3; Thermo Fisher Scientific). For normalization, β-actin was employed as a loading control.

Peptide sequencing

Peptide sequencing analysis was performed by a commercial service provider (ProteinWorks Co., LTD., Republic of Korea). Lyophilized RME powder was dissolved in distilled water to a concentration of 50 mg/mL and centrifuged at 13,000 rpm for 10 min. The supernatant was filtered through a 0.2 μm RC syringe filter and diluted 10-fold with distilled water before LC–MS/MS analysis. Peptide profiling and sequencing were performed using a Vanquish UHPLC system coupled to a Q Exactive Plus mass spectrometer (Thermo Fisher Scientific). Chromatographic separation was carried out using an AdvanceBio Peptide Mapping column (120 Å, 2.1 × 100 mm, 2.7 μm; Agilent Technologies) at 30°C. Mobile phase A consisted of water containing 0.1% formic acid, and mobile phase B consisted of acetonitrile containing 0.1% formic acid. The flow rate was 100 μL/min, and the injection volume was 10 μL. The gradient was as follows: 0–2 min, 2% B; 2–25 min, 2–20% B; 25–30 min, 20–50% B; 30–31 min, 50–98% B; 31–36 min, 98% B; 36–37 min, 98–2% B; and 37–45 min, 2% B. MS and MS/MS analyses were performed in positive ion mode. Full MS scans were acquired over an m/z range of 200–1,500 at a resolution of 70,000, with an AGC target of 3×10^6 and a maximum injection time of 100 ms. Data-dependent MS/MS scans were acquired at a resolution of 17,500, with an AGC target of 1×10^5, a maximum injection time of 100 ms, an isolation window of 1.6 m/z, and normalized collision energy of 25. Peptide sequences were assigned by de novo sequencing. Peptides with 2–15 amino acids were investigated, and 30 peptide sequences were identified from RME. Because de novo sequencing was used, database-dependent false discovery rate values were not calculated. The annotated MS/MS fragmentation spectrum of the selected peptide GEAGPQGARG is provided in Supplementary Fig. S1.

Cell culture, adipocyte differentiation, and peptide treatment

3T3-L1 preadipocytes were obtained from the American Type Culture Collection (ATCC; Manassas, VA, USA) and used as an in vitro adipocyte model. Cells were maintained in Dulbecco's modified Eagle's medium (DMEM; high glucose) supplemented with 10% bovine calf serum and 1% penicillin–streptomycin at 37°C in a humidified atmosphere containing 5% CO_2. For adipogenic differentiation, cells were cultured until reaching confluence. Two days after confluence (designated day 0), differentiation was induced using MDI differentiation medium consisting of DMEM supplemented with 10% fetal bovine serum (FBS), 0.5 mM 3-isobutyl-1-methylxanthine (IBMX), 1 μM dexamethasone, and 10 μg/mL insulin. After 48 h, the medium was replaced with DMEM containing 10% FBS and 10 μg/mL insulin for an additional 48 h. Thereafter, cells were maintained in DMEM containing 10% FBS, and the medium was changed every 2 days until full differentiation. For peptide screening, candidate RME-derived peptides were added during the adipogenic induction period at concentrations of 10, 20, and 50 μM. Specifically, peptides were added to the MDI differentiation medium during the first 48 h of differentiation and were continuously included in the insulin-containing medium for the subsequent 48 h. After the induction period, cells were maintained in DMEM containing 10% FBS without peptide treatment until full differentiation. Cell viability was evaluated in both preadipocytes and differentiated adipocytes. For mechanistic experiments, fully differentiated adipocytes were treated with RMEP-3 at the indicated concentrations for 24 h. To examine the involvement of AMPK signaling, mature adipocytes were pretreated with Compound C (10 μM; Sigma-Aldrich, St. Louis, MO, USA), an AMPK inhibitor, for 1 h prior to RMEP-3 treatment. Compound C was dissolved in dimethyl sulfoxide (DMSO) and diluted in culture medium immediately before use. The final concentration of DMSO was kept below 0.1% in all treatment groups, including the vehicle control. Cells were then incubated with RMEP-3 in the presence or absence of Compound C. A Compound C-only group was included to evaluate the effect of the inhibitor alone. Cell viability under Compound C treatment was also confirmed before mechanistic analysis. Subsequently, the effects of RMEP-3 on thermogenesis-related proteins, including PGC1α and UCP1, and AMPK–ACC signaling were evaluated.

Assessment of lipid accumulation via Oil Red O staining

Intracellular lipid accumulation in mature adipocytes was visualized using Oil Red O staining. Briefly, differentiated cells were washed with PBS and subsequently fixed for 30 min at room temperature in 4% paraformaldehyde. Following the fixation step, the cells were incubated with an Oil Red O working solution for 30 min. After removing the residual stain with several distilled water washes, lipid droplets were imaged via light microscopy. To quantify the lipid content, the stained droplets were dissolved in 100% isopropanol, and the optical density was measured at 520 nm with a microplate reader.

Real-time quantitative PCR

To analyze gene expression, total RNA was isolated from adipose tissues or cultured cells using the TRIzol reagent (Invitrogen, Carlsbad, CA, USA). After assessing the RNA's purity and concentration via spectrophotometry, 2 μg of the RNA was converted into complementary DNA (cDNA) with a High-Capacity cDNA Reverse Transcription Kit (Applied Biosystems, Foster City, CA, USA). Real-time PCR (qPCR) was subsequently executed on an Applied Biosystems platform utilizing SYBR Green Master Mix. The 20-μL reaction volume contained the cDNA, master mix, and target-specific primers. Amplification involved an initial 10-min denaturation at 95 °C, followed by 40 cycles of 95 °C for 15 s and 60 °C for 1 min. Expression levels were normalized to β-actin and calculated through the 2 -△△Ct methodology.

Statistical analysis

Significant differences among the experimental groups were assessed via one-way analysis of variance (ANOVA), with Tukey's post hoc test applied for multiple comparisons. We considered results to be statistically significant when the p-value was below 0.05. The in vivo experiments utilized eight mice per group (n = 8). To confirm the reliability of the in vitro findings, each assay was performed in triplicate and repeated through at least three independent experimental runs.

Results

Rabbit meat extract attenuates body weight gain

Body weight was monitored for 15 weeks to evaluate the anti-obesity effects of RME. Mice maintained on a high-fat diet (HF) displayed a pronounced expansion in body size relative to the control group; however, this increase was visually mitigated in groups receiving RME (Fig. 1A). Temporal body weight changes are shown in Fig. 1B. RME administration suppressed the increase in body weight associated with high-fat feeding, with both RME150 and RME300 groups maintaining lower body weights than the HF group, particularly during the later stages of the experiment. Consistent with these observations, total body weight gain was greater in the HF group than in controls (Fig. 1C), while RME supplementation significantly reduced overall weight gain. Food intake did not differ among groups, indicating that the reduction in body weight was not attributable to changes in energy intake. To further investigate tissue distribution, the weights of major organs and adipose tissues were evaluated (Fig. 1D). Mice maintained on a high-fat diet exhibited significant elevations in the relative mass of the liver, as well as the inguinal and epididymal white adipose tissues (iWAT and eWAT, respectively). In contrast, RME supplementation reduced adipose tissue weights relative to the HF group, indicating reduced adipose tissue accumulation.

Rabbit meat extract mitigates adipocyte hypertrophy and improves serum lipid profiles in obese mice

To investigate whether RME-induced reductions in body weight were accompanied by changes in adipose tissue morphology, histological analysis of eWAT was conducted. Adipocytes from the HF group displayed pronounced hypertrophy, whereas RME-treated groups exhibited visibly smaller adipocytes (Fig. 2A). Quantitative analysis showed that mean adipocyte area was increased in the HF group and reduced following RME supplementation (Fig. 2B). To monitor systemic metabolic shifts, we further analyzed serum lipid profiles. As illustrated in Fig. 2C–F, HF-fed mice displayed elevated concentrations of total cholesterol, triglycerides, HDL cholesterol, and LDL cholesterol relative to the control group. Administration of RME at both 150 and 300 mg/kg reduced serum total cholesterol, triglycerides, and LDL cholesterol levels compared with the HF group. Although HDL cholesterol was slightly reduced in the RME-treated groups, the reductions in total cholesterol, triglycerides, and LDL cholesterol indicate an

overall improvement in obesity-associated dyslipidemia. Nevertheless, the decrease in HDL cholesterol should be interpreted cautiously and warrants further investigation.

Rabbit meat extract attenuates hepatic lipid deposition and reduces serum liver injury markers in high-fat diet-induced obese mice

Hepatic lipid accumulation was assessed through histological examination of liver tissues. As shown in Fig. 3A, the HF group exhibited pronounced lipid accumulation. In contrast, RME-treated groups showed a marked reduction in hepatic lipid deposition, which was confirmed by quantitative analysis of lipid accumulation (Fig. 3B). Hepatic gene expression related to lipogenesis and cholesterol synthesis was further analyzed. Regarding hepatic gene expression, the HF diet upregulated the mRNA levels of key lipogenic and cholesterogenic markers, including *Fasn*, *Scd1*, *Acc1*, *Hmgcr*, and *Hmgcs* (Fig. 3C,D). However, these increases were effectively mitigated by RME supplementation. In parallel, liver injury markers were examined to evaluate hepatic health; while HF feeding led to elevated serum ALT and AST concentrations, RME administration significantly lowered both ALT and AST levels, suggesting attenuation of high-fat diet-associated elevations in serum liver injury markers (Fig. 3E,F).

Rabbit meat extract suppresses adipogenic protein expression and upregulates browning-related markers in adipose tissue

To elucidate the molecular mechanisms underlying RME's anti-obesity effects, we examined protein expression profiles associated with thermogenesis and adipocyte differentiation in fat tissues. Initial analysis of the eWAT revealed that high-fat feeding triggered a marked upregulation of key adipogenic regulators, specifically PPARγ, C/EBPα, and aP2 (Fig. 4A). Notably, this adipogenic induction was blunted by RME treatment. Both the RME150 and RME300 cohorts exhibited a substantial reduction in these markers compared to the HF group, indicating that RME exerts a robust inhibitory influence on the adipogenic program. Furthermore, we examined thermogenesis-related protein expression in the iWAT. RME intervention significantly enhanced the phosphorylation of AMPK compared to the HF-only group (Fig. 4B). In parallel, the expression of PRDM16, PGC1α, and UCP1 was increased in RME-treated

groups. Notably, the RME300 group showed higher levels of these thermogenic markers than the RME150 group, suggesting a dose-dependent response. These results indicate that RME suppresses adipogenic protein expression and increases browning-related marker expression in adipose tissue, which may be associated with AMPK activation.

Compositional characterization of RME

To further characterize RME prepared under the high-temperature, pressurized hot-water extraction condition, extraction yield, total protein content, and free amino acid composition were analyzed. The extraction yield of lyophilized RME was 15% based on the initial raw meat weight. The total protein content of RME was 638 mg/g dry weight, indicating that RME contained abundant water-soluble proteinaceous components. Free amino acid analysis further confirmed the presence of various free amino acids in RME, with L-anserine, L-alanine, L-glutamic acid and glycine being the predominant components (Supplementary Table 1). These results suggest that the extraction process generated or enriched low-molecular-weight nitrogenous compounds, including peptides and free amino acids, in RME.

Identification and screening of peptides derived from rabbit meat extract

Peptide profiling of RME was conducted by LC–MS/MS analysis. The base peak chromatogram (BPC) displayed multiple peptide-related peaks (Fig. 5A), while the extracted ion chromatogram (EIC) confirmed the presence of distinct peptide signals (Fig. 5B). In total, 30 peptide sequences were identified from RME. Hereafter, these peptides were referred to as rabbit meat extract-derived peptides (RMEPs). Several short peptides (2–10 amino acids in length) were selected for subsequent screening. Based on PeptideRanker analysis, five candidate peptides were selected and designated as RMEP-1~RMEP-5 (LR, PLN, GEAGPQGARG, GGRYY, and FAYR). The selected candidate peptides (RMEP-1~RMEP-5) correspond to specific peaks in the EIC as follows: LR (peak 3), PLN (peak 6), GEAGPQGARG (peak 7), GGRYY (peak 16), and FAYR (peak 17) (Fig. 5B). The cytotoxicity of the selected peptides was first evaluated in both preadipocytes and differentiated adipocytes. Treatment with the peptides at

concentrations of 10–50 μM did not affect cell viability, indicating that all peptides were non-toxic within the tested range (Fig. 6A,B). The effects of the peptides on adipocyte differentiation were subsequently evaluated by examining adipogenic marker expression. Of the screened candidates, RMEP-3 (GEAGPQGARG) exhibited the most potent suppressive influence on the transcriptional program of adipogenesis. The anti-adipogenic capacity of RMEP-3 was further evidenced by the profound suppression of the primary adipogenic transcription factors, *PPARγ* and *C/EBPα*, relative to the untreated group (Fig. 6C, D). Concurrently, RMEP-3 administration led to a robust induction of thermogenic gene expression, notably *UCP1* and *PGC1α* (Fig. 6E, F), suggesting increased expression of thermogenesis-related markers. These findings led to the selection of RMEP-3 as the most active peptide for subsequent mechanistic analyses.

Anti-adipogenic effects of RMEP-3 and activation of AMPK signaling

The anti-adipogenic properties of the isolated peptide were further elucidated by evaluating the impact of RMEP-3 on mature adipocytes. Oil Red O staining revealed that RMEP-3 treatment effectively diminished intracellular lipid storage, with a dose-responsive reduction confirmed by quantitative data (Fig. 7A). Furthermore, RMEP-3 triggered the activation of AMPK signaling, evidenced by a significant rise in AMPK phosphorylation (Fig. 7B). Densitometric assessments confirmed a dose-dependent increase in the p-AMPK to total AMPK ratio. This activation was accompanied by the upregulated expression of thermogenic proteins, such as UCP1 and PGC1α (Fig. 7C). In contrast, the levels of the primary adipogenic transcription factors, including PPARγ and C/EBPα, were notably downregulated (Fig. 7D). These results demonstrate that RMEP-3 inhibits adipogenesis while promoting a thermogenic phenotype in adipocytes, potentially through activation of AMPK signaling.

Involvement of the AMPK-ACC signaling axis in the metabolic effects of RMEP-3

To confirm whether the metabolic improvements induced by RMEP-3 are mediated through the AMPK pathway, we utilized Compound C, a well-characterized chemical inhibitor of AMPK signaling. Our results showed that RMEP-3 treatment significantly enhanced AMPK phosphorylation relative to the

MDI-stimulated control (Fig. 8A). This activation was further validated by a corresponding increase in the phosphorylation of acetyl-CoA carboxylase (ACC), which serves as a primary downstream target of AMPK. In contrast, co-treatment with Compound C attenuated the RMEP-3-induced increases in both AMPK and ACC phosphorylation, indicating effective inhibition of AMPK signaling. RMEP-3 treatment significantly upregulated the levels of thermogenic proteins, including PGC1α and UCP1 (Fig. 8B). This induction was partially reversed by Compound C treatment, indicating that the effects of RMEP-3 on thermogenesis-related marker expression are, at least in part, mediated through AMPK activation. These results suggest that RMEP-3-induced regulation of thermogenesis-related proteins is associated, at least in part, with the AMPK–ACC signaling pathway.

Discussion

Our findings demonstrate that RME supplementation effectively mitigated the hallmark features of obesity induced by a high-fat diet, such as accelerated weight gain, hepatic lipid deposition, and enlarged adipocytes. These metabolic improvements were closely linked to a shift in the transcriptional profile of adipose tissues, specifically a reduction in adipogenic regulators and a concurrent induction of markers associated with tissue browning. Notably, LC-MS/MS analysis identified multiple peptides derived from RME, among which a specific peptide (GEAGPQGARG) exhibited potent metabolic regulatory activity in adipocytes. RME and its derived peptide appear to exert complementary roles in the regulation of adipogenesis and energy metabolism. In the present study, hepatic changes were assessed using H&E-based histological observation, serum ALT and AST levels, and hepatic expression of lipogenesis- and cholesterol synthesis-related genes. However, hepatic triglyceride content, Oil Red O staining, inflammatory markers, fibrosis markers, and hepatic insulin signaling were not evaluated. Therefore, the present data support the attenuation of high-fat diet-associated hepatic lipid deposition, serum liver injury marker elevations, and lipogenic gene expression, but they do not establish comprehensive hepatoprotection or full improvement of NAFLD-related pathophysiology. Further studies including hepatic lipid quantification, inflammatory and fibrotic markers, and insulin signaling analysis are required to clarify the broader hepatic effects of RME.

Rabbit meat is recognized as a nutritionally valuable protein source due to its relatively low fat content and balanced fatty acid composition [24,25,27]. Diets rich in lean protein sources are known to improve metabolic health by promoting satiety, enhancing energy expenditure, and regulating lipid metabolism [30–32]. However, despite these nutritional advantages, the metabolic regulatory effects of rabbit meat extracts have not been extensively investigated *in vivo*. Dietary intervention with RME effectively mitigated the systemic metabolic disturbances associated with chronic high-fat consumption, suggesting the potential of RME-derived bioactive constituents as natural modulators of metabolic homeostasis. Excessive adipocyte differentiation and lipid accumulation are characteristic features of obesity [33]. Transcription factors, including C/EBPα and PPARγ, play critical roles in regulating adipogenesis by controlling genes associated with lipid synthesis and adipocyte maturation [34,35]. Consistent with this regulatory framework, rabbit meat extract reduced the expression of these adipogenic markers in adipose tissue, suggesting suppression of adipocyte differentiation. Conversely, thermogenesis-related markers, including UCP1, PRDM16, and PGC1α, were upregulated, suggesting a shift toward a thermogenic phenotype. These proteins are known to regulate mitochondrial activity and thermogenic programming in adipocytes [36,37]. The increased expression of these browning-related markers suggests that rabbit meat extract may suppress adipogenesis while upregulating browning-related marker expression, thereby contributing to changes in adipocyte metabolic regulation. However, these findings should be interpreted as evidence of increased browning-related marker expression rather than definitive proof of functional adipose browning. In the present study, adipose browning was evaluated mainly based on the expression of UCP1, PRDM16, and PGC1α, whereas additional histological and functional analyses, such as UCP1 immunohistochemistry, evaluation of multilocular beige adipocyte morphology, mitochondrial DNA content, oxygen consumption rate, thermogenic capacity, and cold-challenge experiments, were not performed. Therefore, further studies are required to determine whether RME induces functional adipose browning in vivo.

Serving as a pivotal mediator of cellular energy balance, AMP-activated protein kinase (AMPK) orchestrates various metabolic processes dedicated to energy consumption [9]. The stimulation of AMPK is widely recognized for its ability to bolster mitochondrial function and amplify energy expenditure.

Concurrently, it exerts inhibitory control over adipogenic differentiation and lipid buildup, while also acting as a primary trigger for the browning of adipose tissue [38,39]. In line with these roles, both RME and the identified peptide increased AMPK phosphorylation, suggesting involvement of AMPK signaling in their metabolic effects. These observations further implicate AMPK as a key pathway associated with the regulatory actions of RME on adipocyte metabolism and energy balance.

The extraction condition used in this study was intended to reflect a conventional high-temperature, pressurized hot-water extraction process for meat-based extract or decoction-type food products. Under this condition, 120°C at 30 psi for 12 h, protein denaturation, peptide release, and the formation of low-molecular-weight nitrogenous compounds may occur. Consistent with this, lyophilized RME showed an extraction yield of 15% and a total protein content of 638 mg/g dry weight, together with detectable levels of various free amino acids. Therefore, the peptide profile identified in this study should be interpreted as representing peptides generated or enriched under the specific thermal extraction condition, rather than peptides naturally present in raw rabbit meat. In addition, the serve thermal extraction condition used in this study may have promoted the formation of Maillard reaction-derived compounds, including advanced glycation end products (AGEs) and hydroxymethylfurfural (HMF). Because AGEs, HMF, and other Maillard-derived products were not quantified in the present study, their possible contribution to the biological activity or compositional characteristics of RME cannot be excluded. This represents a limitation of the present study, and future studies should quantify heat-induced Maillard reaction products to better characterize RME prepared under high-temperature extraction conditions. In addition, peptide content, lipid content, ash content, molecular weight distribution, and batch-to-batch variability were not fully quantified in the present study. Therefore, more comprehensive compositional profiling and batch standardization will be required in future studies to improve dose interpretation, reproducibility, and industrial applicability of RME.

Bioactive peptides derived from food proteins exhibit diverse physiological functions and have been explored for their metabolic regulatory potential. Peptides originating from sources such as collagen, milk,

and fish proteins have been shown to improve lipid metabolism and inhibit adipocyte differentiation [40-42]. Although several food-derived peptides have been investigated for their metabolic effects, information on rabbit meat-derived peptides and their roles in adipocyte metabolism remains limited. In this study, LC-MS/MS analysis combined with de novo sequencing identified several peptides from rabbit meat extract. Functional screening of these peptides revealed that GEAGPQGARG exhibited the strongest anti-adipogenic activity in adipocytes, as evidenced by reduced lipid accumulation, suppression of adipogenic gene expression, and increased expression of thermogenic markers. A UniProt-based sequence similarity search was performed to predict the putative parent protein of GEAGPQGARG. The peptide contains a Gly-rich sequence pattern, including a Gly–X–Y-like motif, which is characteristic of collagen-derived peptides. The search results suggested that GEAGPQGARG may originate from collagen α-chain proteins, particularly type I collagen α1/α2 chains. This interpretation is consistent with previous studies showing that collagen-derived peptides, including fish collagen peptides, can regulate lipid metabolism, suppress adipocyte differentiation, and improve obesity-related metabolic parameters [40]. In the present study, GEAGPQGARG reduced adipogenic marker expression and increased thermogenic markers in adipocytes, suggesting that rabbit meat-derived collagen-like peptides may contribute to the metabolic regulatory activity of RME. However, the in vivo relevance of GEAGPQGARG remains to be confirmed. In the present study, the anti-obesity effects observed in animals were induced by oral administration of whole RME, whereas GEAGPQGARG was evaluated only in cultured adipocytes. Therefore, the in vivo effects of RME cannot be attributed solely to GEAGPQGARG. It remains unknown whether GEAGPQGARG is stable during gastrointestinal digestion, absorbed intact, detectable in circulation, delivered to adipose tissue, or capable of reproducing the anti-obesity effects of whole RME in vivo. Future studies should include oral administration of synthetic GEAGPQGARG in diet-induced obesity models, simulated gastrointestinal digestion, targeted LC–MS/MS-based detection of the peptide in plasma and adipose tissue, and pharmacokinetic and tissue distribution analyses to confirm its bioavailability and in vivo functional relevance. Thus, this study provides preliminary evidence that a rabbit meat-derived peptide can modulate adipocyte metabolism

through AMPK-associated signaling pathways, while further in vivo validation is required to establish its physiological relevance.

From an animal science perspective, the characteristics of rabbit meat raw materials, including breed, sex, age, anatomical cut, rearing environment, and post-mortem handling conditions, may affect protein composition, peptide generation, and biological activity. In the present study, RME was prepared using commercially processed rabbit meat purchased from the Korea Rabbit and Deer Agricultural Cooperative; therefore, detailed production-related information was limited. This represents a limitation of the present study. Future studies using standardized rabbit meat materials with controlled breed, age, sex, anatomical cut, and post-mortem aging conditions are required to improve reproducibility and support industrial application. Another limitation of the present study is the lack of comparative data using extracts from other livestock species or a positive control compound. Although RME showed anti-obesity activity under the present experimental conditions, the current data do not demonstrate that rabbit meat is superior to other livestock-derived protein sources. In this study, extracts from chicken, pork, or other livestock species prepared under identical extraction conditions were not included, and a positive control was not used. Therefore, future studies should compare RME with extracts from other livestock species prepared under standardized conditions and include appropriate positive controls to clarify the relative functional advantage and industrial applicability of rabbit meat-derived bioactive peptides. To further assess the practical relevance of the administered doses, the human equivalent dose (HED) was estimated using the body surface area-based conversion method. The HED was calculated as follows: HED (mg/kg) = animal dose (mg/kg) × animal Km/human Km. Using Km values of 3 for mice and 37 for humans, the mouse doses of 150 and 300 mg/kg correspond to HED values of approximately 12.2 and 24.3 mg/kg, respectively, equivalent to approximately 0.73 and 1.46 g/day for a 60-kg adult. These estimated intake levels suggest that RME may be feasible as a food-derived functional ingredient. However, further studies, including human trials and safety evaluations, are required to confirm its effective intake range and practical applicability.

Conclusion

RME attenuated obesity-related phenotypes in a high-fat diet model, reducing body weight gain, adiposity, and hepatic lipid accumulation, while improving serum lipid profiles. These metabolic improvements were associated with suppression of adipogenic markers and upregulation of browning-related proteins in adipose tissue, accompanied by increased AMPK phosphorylation. Furthermore, LC–MS/MS analysis identified several peptides derived from RME, among which one peptide (GEAGPQGARG) exhibited significant metabolic regulatory effects by suppressing adipogenic factors and enhancing thermogenic markers in adipocytes. Collectively, these findings suggest that RME may serve as a promising functional food resource for obesity management, while GEAGPQGARG represents an in vitro active candidate peptide that requires further in vivo validation.

Acknowledgments

This research work was carried out with the support of "Cooperative Research Program for Agriculture Science and Technology Development (Project No. RS-2022-RD010371)" Rural Development Administration, Korea.

References

1. Li J, Li Y, Zhou X, Yang S, Liu D, Wen H, Chen X, Duan C, Yu M, Zhang M, Tang B, Wang Y, Wang L, Wu Y. Adipocytes orchestrate obesity-related chronic inflammation through β2-microglobulin. Signal Transduct Target Ther. 2025 Dec 3;10(1):394. doi: 10.1038/s41392-025-02486-3. PMID: 41330906; PMCID: PMC12672573.
2. Młynarska E, Bojdo K, Bulicz A, Frankenstein H, Gąsior M, Kustosik N, Rysz J, Franczyk B. Obesity as a Multifactorial Chronic Disease: Molecular Mechanisms, Systemic Impact, and Emerging Digital Interventions. Curr Issues Mol Biol. 2025 Sep 23;47(10):787. doi: 10.3390/cimb47100787. PMID: 41150735; PMCID: PMC12564886.

3. Moschonis G, Trakman GL. Overweight and Obesity: The Interplay of Eating Habits and Physical Activity. Nutrients. 2023 Jun 27;15(13):2896. doi: 10.3390/nu15132896. PMID: 37447222; PMCID: PMC10343820.
4. Ahmed SK, Mohammed RA. Obesity: Prevalence, causes, consequences, management, preventive strategies and future research directions. Metabol Open. 2025 Jun 14;27:100375. doi: 10.1016/j.metop.2025.100375. PMID: 41041606; PMCID: PMC12486175.
5. Bae YA, Cheon HG. Adipocyte Browning: A Promising Avenue in Anti-Obesity Therapy. Int J Mol Sci. 2026 Jan 28;27(3):1321. doi: 10.3390/ijms27031321. PMID: 41683747; PMCID: PMC12898576.
6. Kuryłowicz A, Puzianowska-Kuźnicka M. Induction of Adipose Tissue Browning as a Strategy to Combat Obesity. Int J Mol Sci. 2020 Aug 28;21(17):6241. doi: 10.3390/ijms21176241. PMID: 32872317; PMCID: PMC7504355.
7. Zhu Y, Liu W, Qi Z. Adipose tissue browning and thermogenesis under physiologically energetic challenges: a remodelled thermogenic system. J Physiol. 2024 Jan;602(1):23-48. doi: 10.1113/JP285269. Epub 2023 Nov 29. PMID: 38019069.
8. Kajimura S, Spiegelman BM, Seale P. Brown and Beige Fat: Physiological Roles beyond Heat Generation. Cell Metab. 2015 Oct 6;22(4):546-59. doi: 10.1016/j.cmet.2015.09.007. PMID: 26445512; PMCID: PMC4613812.
9. Wu L, Zhang L, Li B, Jiang H, Duan Y, Xie Z, Shuai L, Li J, Li J. AMP-Activated Protein Kinase (AMPK) Regulates Energy Metabolism through Modulating Thermogenesis in Adipose Tissue. Front Physiol. 2018 Feb 21;9:122. doi: 10.3389/fphys.2018.00122. PMID: 29515462; PMCID: PMC5826329.
10. Ahmad B, Serpell CJ, Fong IL, Wong EH. Molecular Mechanisms of Adipogenesis: The Anti-adipogenic Role of AMP-Activated Protein Kinase. Front Mol Biosci. 2020 May 8;7:76. doi: 10.3389/fmolb.2020.00076. PMID: 32457917; PMCID: PMC7226927.

11. Desjardins EM, Steinberg GR. Emerging Role of AMPK in Brown and Beige Adipose Tissue (BAT): Implications for Obesity, Insulin Resistance, and Type 2 Diabetes. Curr Diab Rep. 2018 Aug 17;18(10):80. doi: 10.1007/s11892-018-1049-6. PMID: 30120579.
12. Ignot-Gutiérrez A, Serena-Romero G, Guajardo-Flores D, Alvarado-Olivarez M, Martínez AJ, Cruz-Huerta E. Proteins and Peptides from Food Sources with Effect on Satiety and Their Role as Anti-Obesity Agents: A Narrative Review. Nutrients. 2024 Oct 20;16(20):3560. doi: 10.3390/nu16203560. PMID: 39458554; PMCID: PMC11510221.
13. Hajfathalian M, Ghelichi S, Jacobsen C. Anti-obesity peptides from food: Production, evaluation, sources, and commercialization. Compr Rev Food Sci Food Saf. 2025 Mar;24(2):e70158. doi: 10.1111/1541-4337.70158. PMID: 40111015; PMCID: PMC11924896.
14. Chakrabarti S, Jahandideh F, Wu J. Food-derived bioactive peptides on inflammation and oxidative stress. Biomed Res Int. 2014;2014:608979. doi: 10.1155/2014/608979. Epub 2014 Jan 2. PMID: 24527452; PMCID: PMC3914560.
15. Singh BP, Aluko RE, Hati S, Solanki D. Bioactive peptides in the management of lifestyle-related diseases: Current trends and future perspectives. Crit Rev Food Sci Nutr. 2022;62(17):4593-4606. doi: 10.1080/10408398.2021.1877109. Epub 2021 Jan 28. PMID: 33506720.
16. Garcés-Rimón M, Morales D, Miguel-Castro M. Potential Role of Bioactive Proteins and Peptides Derived from Legumes towards Metabolic Syndrome. Nutrients. 2022 Dec 10;14(24):5271. doi: 10.3390/nu14245271. PMID: 36558429; PMCID: PMC9782127.
17. Patil P, Mandal S, Tomar SK, Anand S. Food protein-derived bioactive peptides in management of type 2 diabetes. Eur J Nutr. 2015 Sep;54(6):863-80. doi: 10.1007/s00394-015-0974-2. Epub 2015 Jul 8. PMID: 26154777.
18. Zhao M, Qiao K, Zhang L, Liang L, Chen S, Chen L, Zhang Y. Research Progress on Anti-Hyperlipidemia Peptides Derived from Foods. Nutrients. 2025 Mar 28;17(7):1181. doi: 10.3390/nu17071181. PMID: 40218939; PMCID: PMC11990363.

19. D'Souza K, Mercer A, Mawhinney H, Pulinilkunnil T, Udenigwe CC, Kienesberger PC. Whey Peptides Stimulate Differentiation and Lipid Metabolism in Adipocytes and Ameliorate Lipotoxicity-Induced Insulin Resistance in Muscle Cells. Nutrients. 2020 Feb 6;12(2):425. doi: 10.3390/nu12020425. PMID: 32041341; PMCID: PMC7071342.
20. Udenigwe CC, Rouvinen-Watt K. The Role of Food Peptides in Lipid Metabolism during Dyslipidemia and Associated Health Conditions. Int J Mol Sci. 2015 Apr 24;16(5):9303-13. doi: 10.3390/ijms16059303. PMID: 25918936; PMCID: PMC4463589.
21. Wang S, Moustaid-Moussa N, Chen L, Mo H, Shastri A, Su R, Bapat P, Kwun I, Shen CL. Novel insights of dietary polyphenols and obesity. J Nutr Biochem. 2014 Jan;25(1):1-18. doi: 10.1016/j.jnutbio.2013.09.001. PMID: 24314860; PMCID: PMC3926750.
22. Zhu W, Oteiza PI. Proanthocyanidins at the gastrointestinal tract: mechanisms involved in their capacity to mitigate obesity-associated metabolic disorders. Crit Rev Food Sci Nutr. 2024;64(2):220-240. doi: 10.1080/10408398.2022.2105802. Epub 2022 Aug 9. PMID: 35943169.
23. Shang A, Li J, Zhou DD, Gan RY, Li HB. Molecular mechanisms underlying health benefits of tea compounds. Free Radic Biol Med. 2021 Aug 20;172:181-200. doi: 10.1016/j.freeradbiomed.2021.06.006. Epub 2021 Jun 10. PMID: 34118386.
24. Dalle Zotte A, Szendro Z. The role of rabbit meat as functional food. Meat Sci. 2011 Jul;88(3):319-31. doi: 10.1016/j.meatsci.2011.02.017. Epub 2011 Feb 24. PMID: 21392894.
25. Cullere M, Dalle Zotte A. Rabbit meat production and consumption: State of knowledge and future perspectives. Meat Sci. 2018 Sep;143:137-146. doi: 10.1016/j.meatsci.2018.04.029. Epub 2018 Apr 28. PMID: 29751220.
26. Kumar SA, Kim HJ, Jayasena DD, Jo C. On-Farm and Processing Factors Affecting Rabbit Carcass and Meat Quality Attributes. Food Sci Anim Resour. 2023 Mar;43(2):197-219. doi: 10.5851/kosfa.2023.e5. Epub 2023 Mar 1. PMID: 36909860; PMCID: PMC9998196

27. Mancini S, Mattioli S, Dal Bosco A. Rabbit meat quality with an approach to its processing using spices or specific ingredients as antioxidants. World Rabbit Sci. 2025;33(2):93-102. doi: 10.4995/wrs.2025.22656.

28. Kumar P, Sharma N, Narnoliya LK, Verma AK, Umaraw P, Mehta N, Ismail-Fitry MR, Kaka U, Yong-Meng G, Lee SJ, Sazili AQ. Improving quality and consumer acceptance of rabbit meat: Prospects and challenges. Meat Sci. 2025 Jan;219:109660. doi: 10.1016/j.meatsci.2024.109660. Epub 2024 Sep 14. PMID: 39312855.

29. Plotuna AM, Hotea I, Tîrziu E. Improving the Nutritional Properties of Rabbit Meat Through Dietary Supplementation with Linseed Meal, Fodder Yeast, and Selenium Yeast. Appl Sci. 2025;15(10):5427. doi: 10.3390/app15105427.

30. Westerterp-Plantenga MS, Lemmens SG, Westerterp KR. Dietary protein - its role in satiety, energetics, weight loss and health. Br J Nutr. 2012 Aug;108 Suppl 2:S105-12. doi: 10.1017/S0007114512002589. PMID: 23107521.

31. Halton TL, Hu FB. The effects of high protein diets on thermogenesis, satiety and weight loss: a critical review. J Am Coll Nutr. 2004 Oct;23(5):373-85. doi: 10.1080/07315724.2004.10719381. PMID: 15466943.

32. Li J, Armstrong CL, Campbell WW. Effects of Dietary Protein Source and Quantity during Weight Loss on Appetite, Energy Expenditure, and Cardio-Metabolic Responses. Nutrients. 2016 Jan 26;8(2):63. doi: 10.3390/nu8020063. PMID: 26821042; PMCID: PMC4772027.

33. Ruiz-Ojeda FJ, Rupérez AI, Gomez-Llorente C, Gil A, Aguilera CM. Cell Models and Their Application for Studying Adipogenic Differentiation in Relation to Obesity: A Review. Int J Mol Sci. 2016 Jun 30;17(7):1040. doi: 10.3390/ijms17071040. PMID: 27376273; PMCID: PMC4964416.

34. Farmer SR. Transcriptional control of adipocyte formation. Cell Metab. 2006 Oct;4(4):263-73. doi: 10.1016/j.cmet.2006.07.001. PMID: 17011499; PMCID: PMC1958996.

35. Lee JE, Schmidt H, Lai B, Ge K. Transcriptional and Epigenomic Regulation of Adipogenesis. Mol Cell Biol. 2019 May 14;39(11):e00601-18. doi: 10.1128/MCB.00601-18. PMID: 30936246; PMCID: PMC6517598.

36. Seale P. Transcriptional control of brown adipocyte development and thermogenesis. Int J Obes (Lond). 2010 Oct;34 Suppl 1:S17-22. doi: 10.1038/ijo.2010.178. PMID: 20935660.

37. Gill JA, La Merrill MA. An emerging role for epigenetic regulation of Pgc-1α expression in environmentally stimulated brown adipose thermogenesis. Environ Epigenet. 2017 Jun 30;3(2):dvx009. doi: 10.1093/eep/dvx009. PMID: 29492311; PMCID: PMC5804549.

38. Yuan J, Nian Y, Wang X, Shi Q, Shui S, Cai H, Lin Y, Zhang X, Wang F, Chen J, Qiu M, Liu J. Actein ameliorates diet-induced obesity through the activation of AMPK-mediated white fat browning. Phytomedicine. 2024 Nov;134:156009. doi: 10.1016/j.phymed.2024.156009. Epub 2024 Aug 30. PMID: 39260136.

39. Wang Q, Sun J, Liu M, Zhou Y, Zhang L, Li Y. The New Role of AMP-Activated Protein Kinase in Regulating Fat Metabolism and Energy Expenditure in Adipose Tissue. Biomolecules. 2021 Nov 24;11(12):1757. doi: 10.3390/biom11121757. PMID: 34944402; PMCID: PMC8698496.

40. Lee EJ, Hur J, Ham SA, Jo Y, Lee S, Choi MJ, Seo HG. Fish collagen peptide inhibits the adipogenic differentiation of preadipocytes and ameliorates obesity in high fat diet-fed mice. Int J Biol Macromol. 2017 Nov;104(Pt A):281-286. doi: 10.1016/j.ijbiomac.2017.05.151. Epub 2017 Jun 9. PMID: 28602994.

41. Woo M, Noh JS. Regulatory Effects of Skate Skin-Derived Collagen Peptides with Different Molecular Weights on Lipid Metabolism in the Liver and Adipose Tissue. Biomedicines. 2020 Jun 30;8(7):187. doi: 10.3390/biomedicines8070187. PMID: 32630126; PMCID: PMC7400643.

42. Pueyo-Arias M, López-Yoldi M, Navas-Carretero S, González-Navarro CJ, Zulet MLÁ, Milagro FI. Collagen supplementation in metabolic syndrome: a narrative review unraveling the biological mechanisms and effects. Nutr Res Rev. 2025 Dec 22;39:e10. doi: 10.1017/S0954422425100309. PMID: 41424065.

Figure Legend

Fig. 1

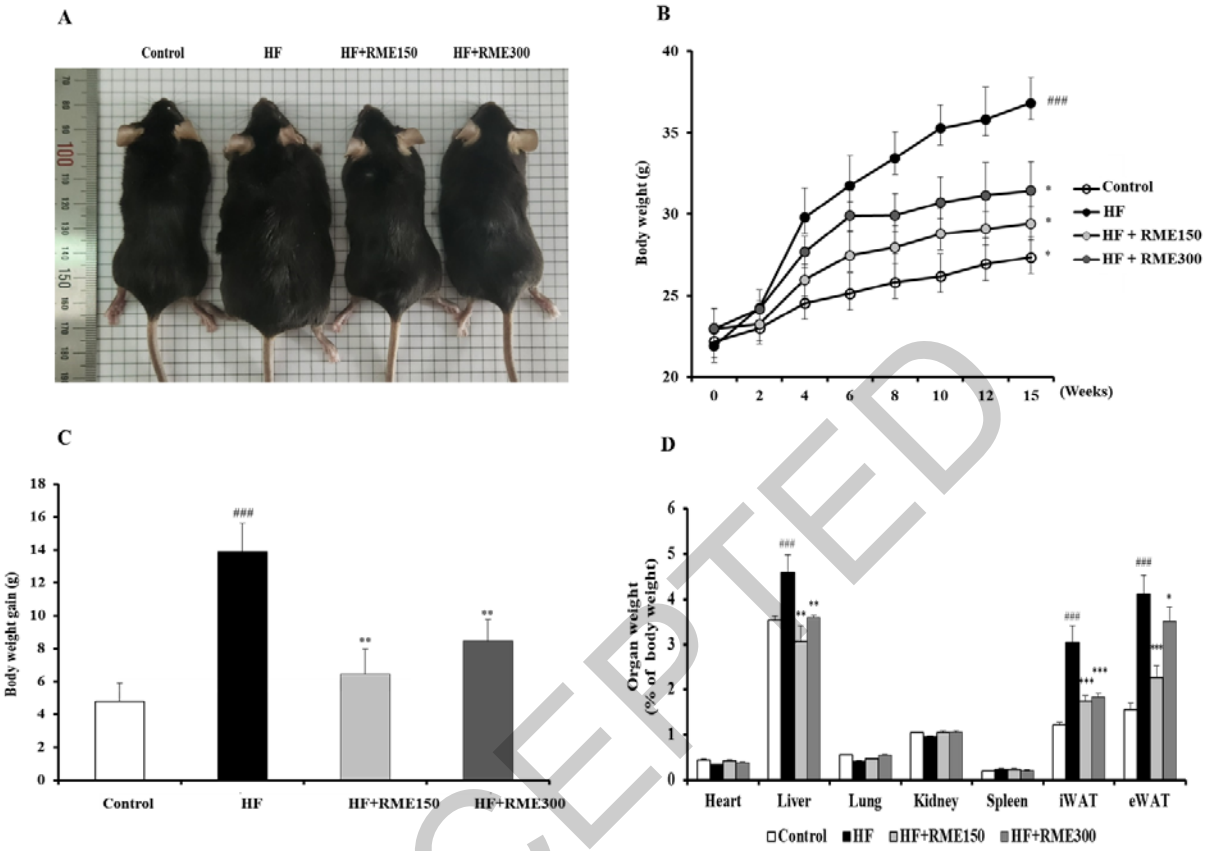

Figure 1. Effects of RME on body weight and organ weights in high-fat diet-induced obese mice. (A) Representative images of mice from each experimental group after 15 weeks of dietary intervention. (B) Body weight changes during the experimental period. (C) Final body weight at the end of the experiment. (D) Organ weights measured at sacrifice. Data are expressed as mean ± SEM (n = 8 per group). ###p <0.001 vs. control group; *p < 0.05, **p < 0.01, ***p < 0.001 vs. HF group.

Fig. 2

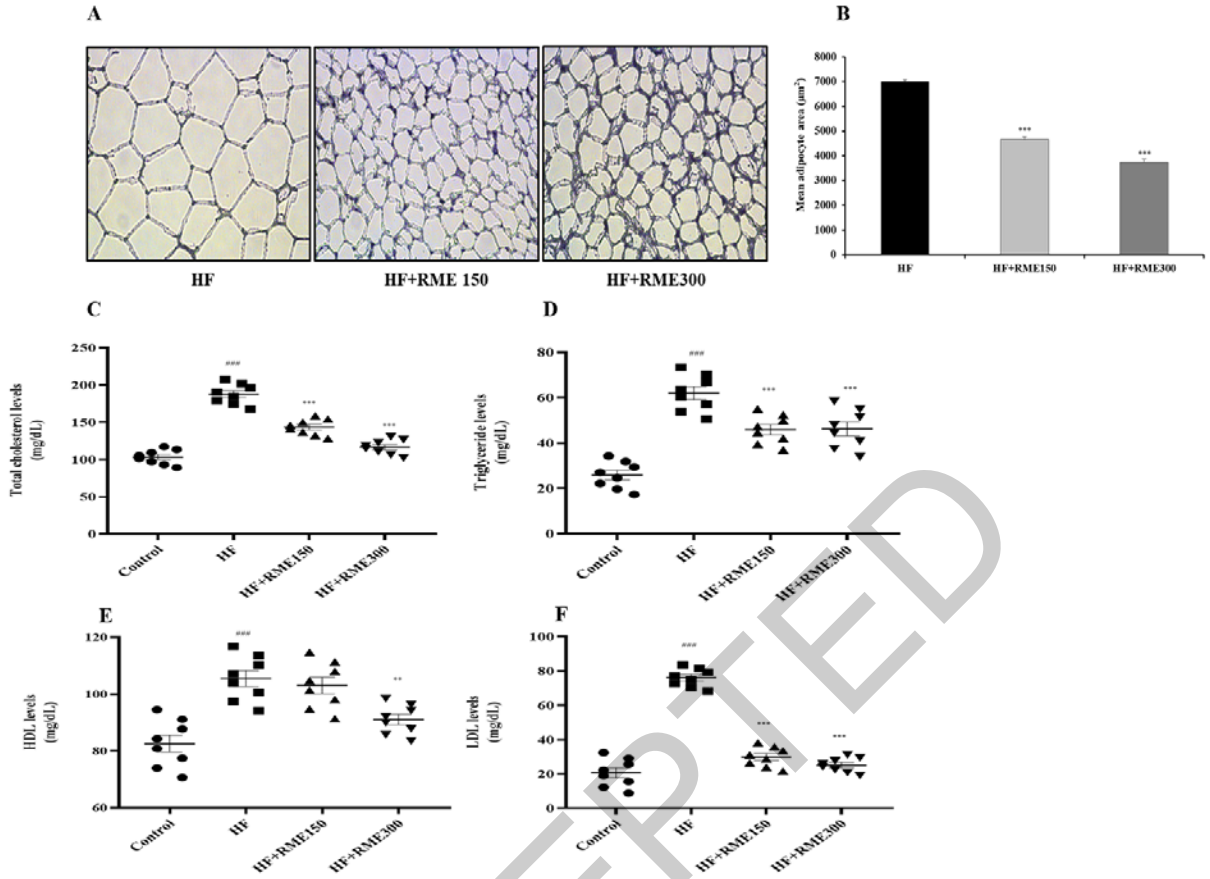

Figure 2. Effects of RME on adipocyte morphology and serum lipid profiles in high-fat diet-induced obese mice.

(A) Representative H&E staining of eWAT. (B) Quantification of adipocyte area. (C–F) Serum lipid parameters, including total cholesterol (C), triglycerides (D), HDL (E), and LDL (F). Data are expressed as mean ± SEM (n = 8 per group). For serum lipid parameters, individual data points are overlaid on the graph. ###p <0.001 vs. control group; **p < 0.01, ***p < 0.001 vs. HF group.

Fig. 3

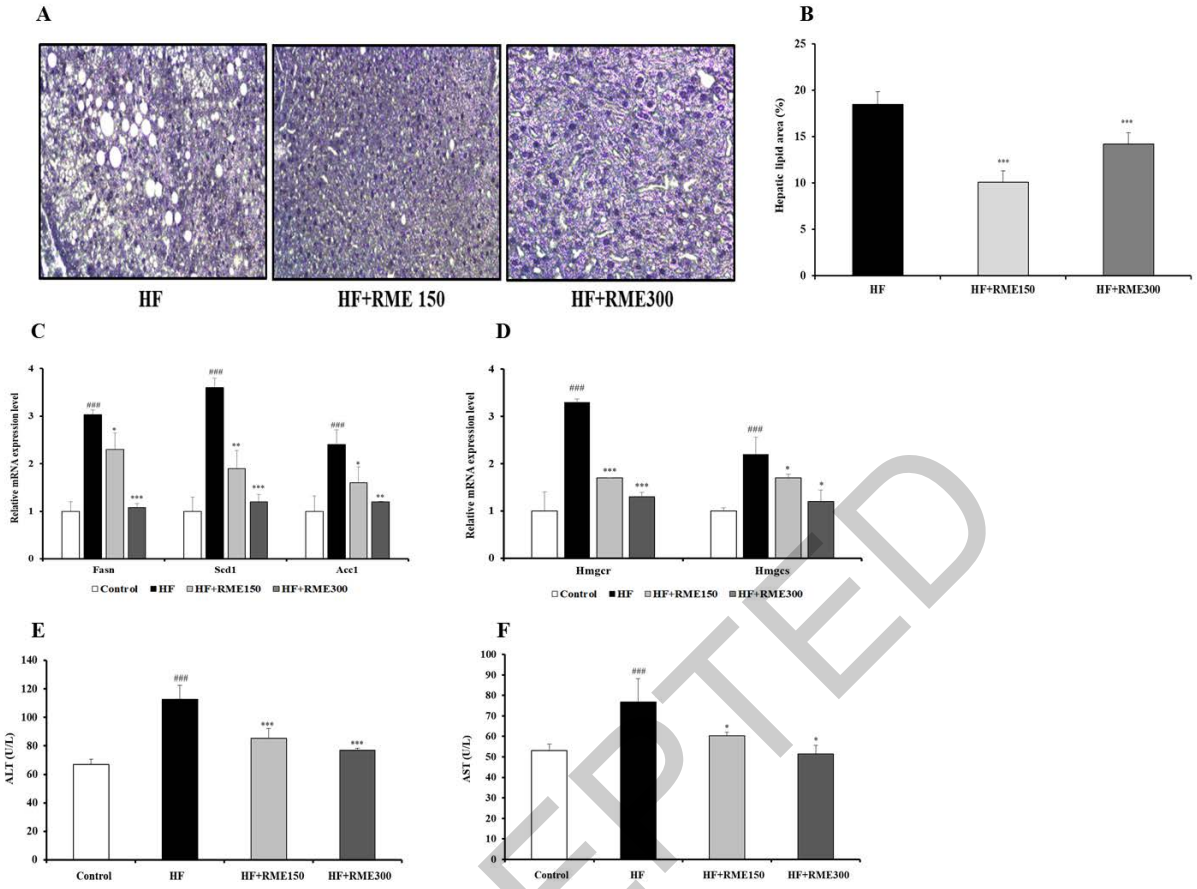

Figure 3. Effects of RME on hepatic lipid deposition, lipid metabolism–related gene expression, and serum liver injury markers in high-fat diet-induced obese mice.

(A) Representative H&E staining of liver sections. (B) Quantification of hepatic lipid accumulation. (C, D) Relative mRNA expression levels of lipid metabolism–related genes, including Fasn, Scd1, Acc1, Hmgcr, and Hmgcs. (E, F) ALT and AST levels. Data are expressed as mean ± SEM (n = 8 per group). ###p <0.001 vs. control group; *p < 0.05, **p < 0.01, ***p < 0.001 vs. HF group.

Fig. 4

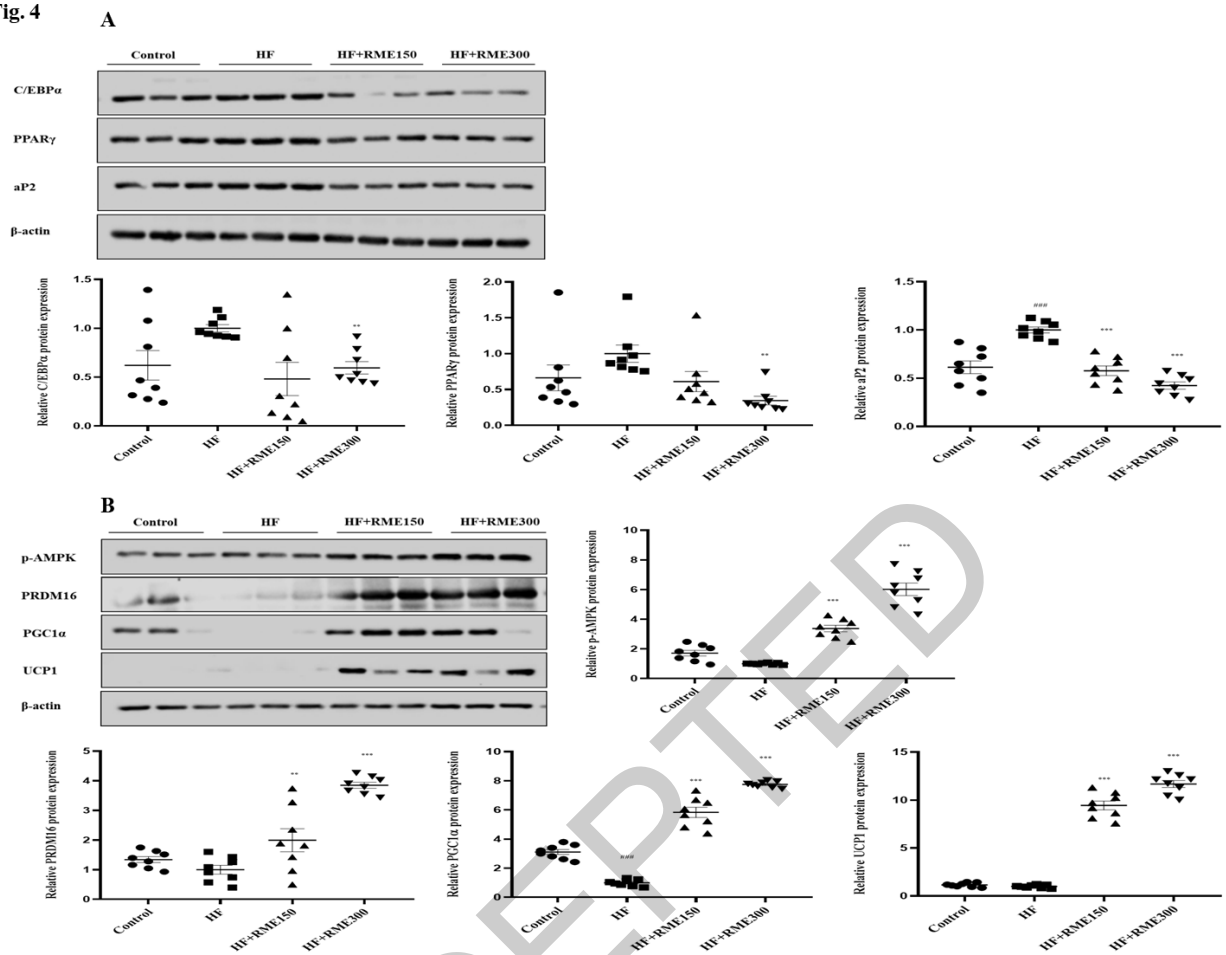

Figure 4. Effects of RME on adipogenesis- and thermogenesis-related protein expression in adipose tissues of high-fat diet-induced obese mice.

(A) Representative western blot images and quantification of adipogenic proteins, including C/EBPα, PPARγ, and aP2, in eWAT. (B) Representative western blot images and quantification of p-AMPK, PRDM16, PGC1α, and UCP1 in iWAT. Protein expression levels were normalized to β-actin. Quantitative data are expressed as mean ± SEM with individual data points overlaid (n = 8 per group). $^{**}p < 0.01$, $^{***}p < 0.001$ vs. HF group.

Fig. 5

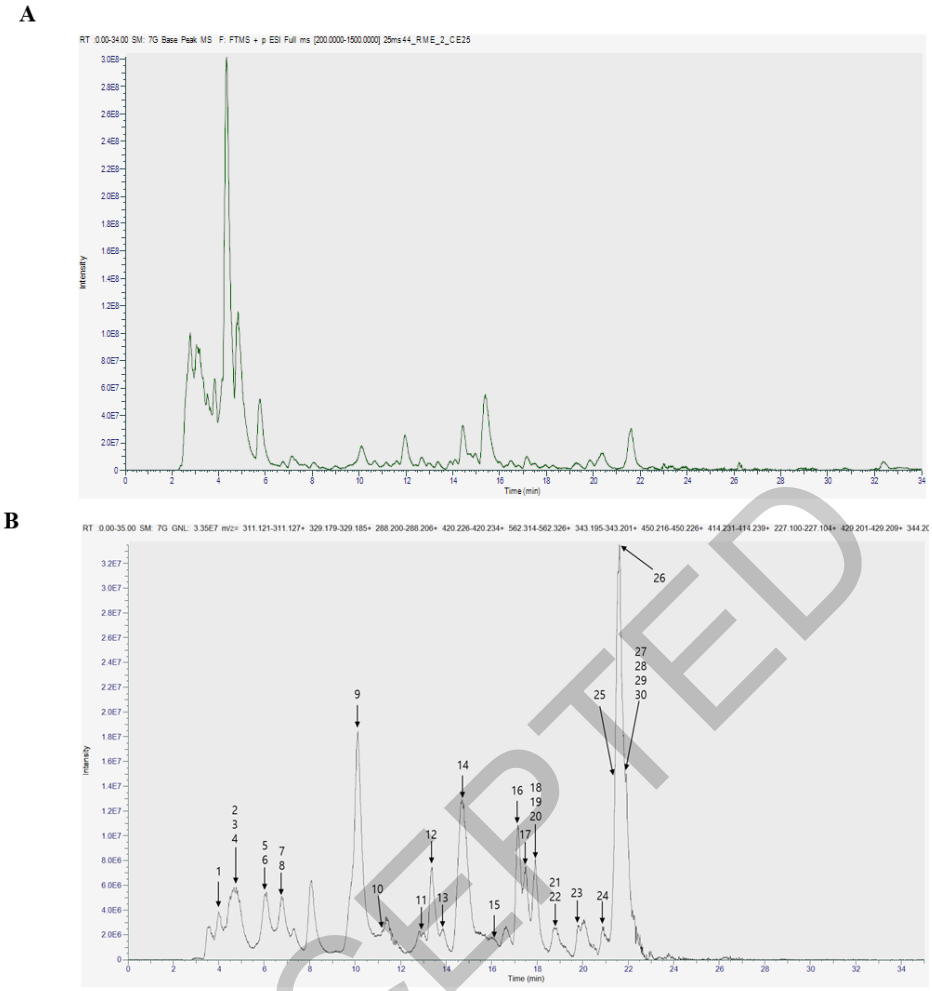

Figure 5. LC–MS/MS-based peptide profiling of rabbit meat extract (RME).

(A) Base peak chromatogram (BPC) of RME obtained by LC–MS/MS analysis. (B) Extracted ion chromatogram (EIC) showing representative peptide-associated ion signals. LC–MS/MS analysis was performed to identify peptide components present in RME. The BPC demonstrates the overall distribution of peptide-related peaks, while the EIC confirms the presence of distinct peptide signals within the extract.

Fig. 6

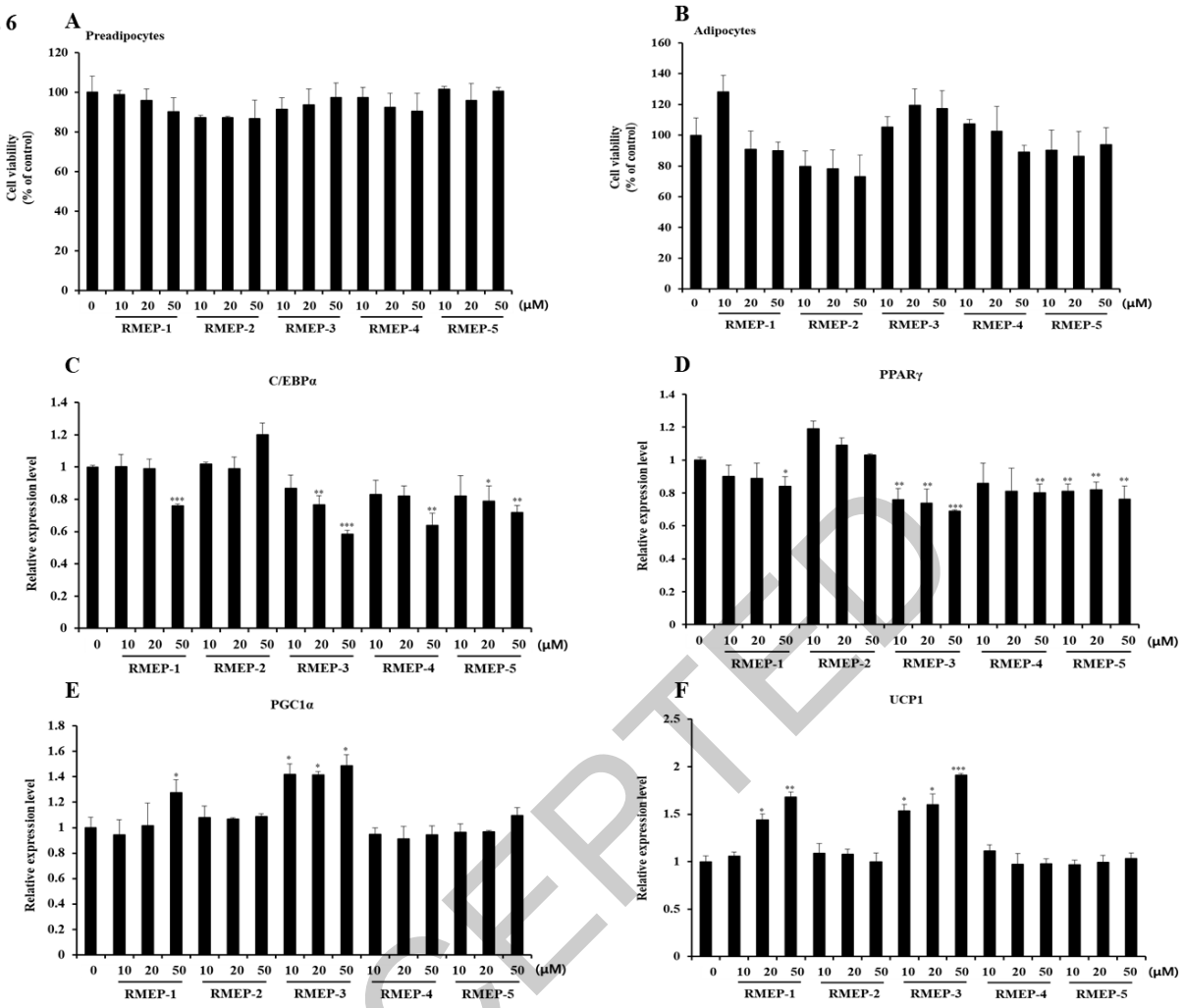

Figure 6. Screening and identification of bioactive peptides derived from RME.

(A, B) Cell viability of preadipocytes (A) and differentiated adipocytes (B) following treatment with candidate peptides at concentrations of 10, 20, and 50 μM. (C, D) Relative mRNA expression levels of adipogenic markers, including C/EBPα (C) and PPARγ (D). (E, F) Relative mRNA expression levels of thermogenesis-related genes, including PGC1α (E) and UCP1 (F). Cells were treated with candidate peptides (10–50 μM), and gene expression levels were normalized to an internal control. Data are expressed as mean ± SD from three independent experiments. *$p < 0.05$, **$p < 0.01$, ***$p < 0.001$ vs. control group.

Fig. 7

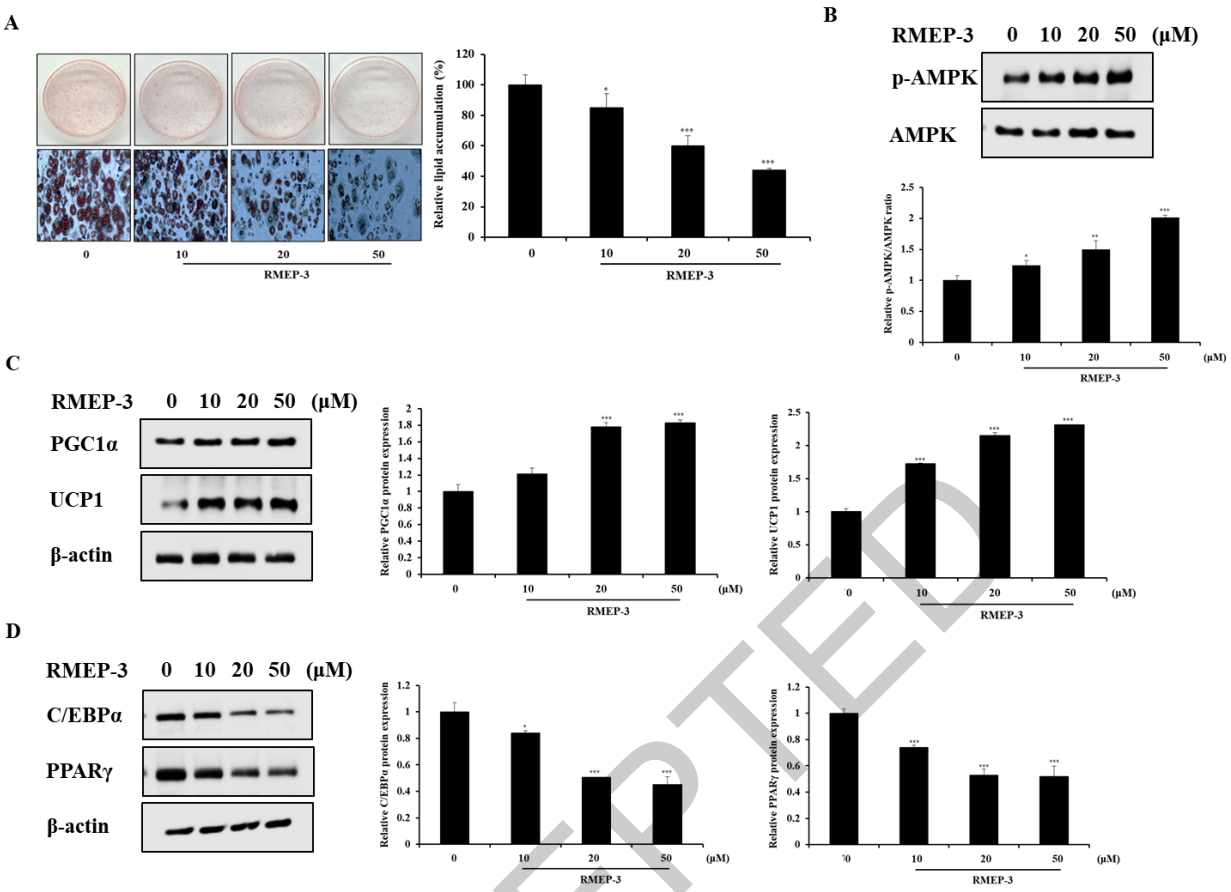

Figure 7. Effects of the selected peptide RMEP-3 on lipid accumulation, AMPK activation, and adipogenesis- and thermogenesis-related protein expression in adipocytes.

(A) Representative Oil Red O staining and quantitative analysis of lipid accumulation in adipocytes treated with RMEP-3 (0, 10, 20, and 50 μM). (B) Representative western blot images and quantification of p-AMPK and total AMPK. (C) Representative western blot images and quantification of thermogenesis-related proteins, including PGC1α and UCP1. (D) Representative western blot images and quantification of adipogenic proteins, including C/EBPα and PPARγ. Cells were treated with RMEP-3 at the indicated concentrations (0–50 μM). Protein expression levels were normalized to β-actin, and the p-AMPK/AMPK ratio was calculated. Data are expressed as mean ± SD from three independent experiments. *$p < 0.05$, ***$p < 0.001$ vs. control group.

Fig. 8

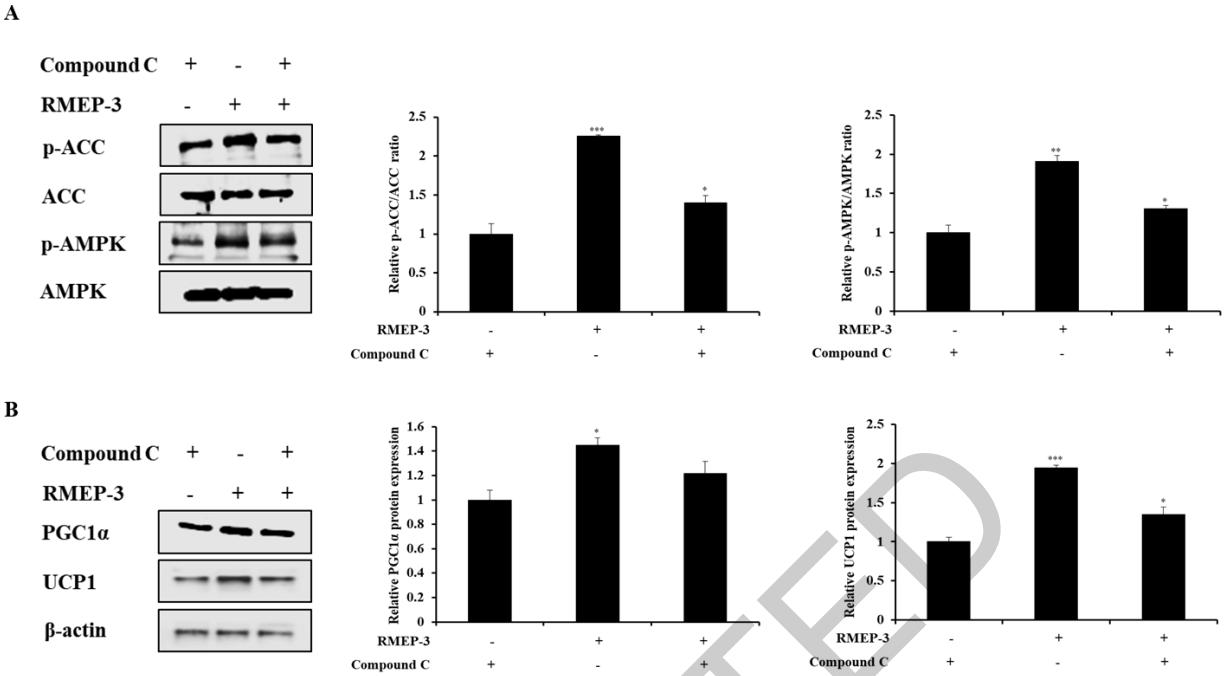

Figure 8. Involvement of AMPK signaling in the metabolic effects of RMEP-3 in adipocytes.

(A) Representative western blot images and quantification of phosphorylated AMP-activated protein kinase (p-AMPK), total AMPK, phosphorylated acetyl-CoA carboxylase (p-ACC), and total ACC. (B) Representative western blot images and quantification of thermogenesis-related proteins, including peroxisome proliferator-activated receptor gamma coactivator 1 alpha (PGC1α) and uncoupling protein 1 (UCP1). Adipocytes were treated with differentiation medium (MDI), RMEP-3, or RMEP-3 in combination with Compound C (AMPK inhibitor). Protein expression levels were normalized to β-actin, and the p-AMPK/AMPK and p-ACC/ACC ratios were calculated. Data are expressed as mean ± SD from three independent experiments. *p < 0.05, **p < 0.01, ***p < 0.001 vs. MDI group.

Figures

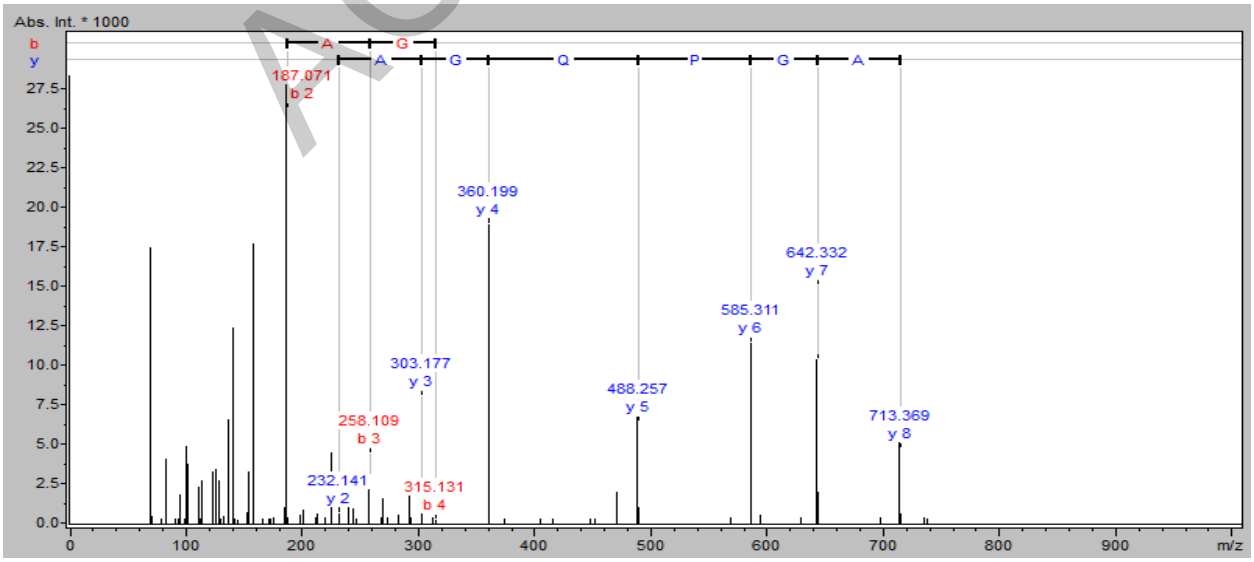

Supplementary Fig. S1. Annotated MS/MS fragmentation spectrum of GEAGPQGARG identified from rabbit meat extract (RME). The peptide was detected at RT 6.6 min with a precursor ion of m/z 450.221 (z = 2) and a calculated molecular mass of 899.435 Da. Matched b- and y-ion series supported the de novo assignment of the GEAGPQGARG sequence.

Supplementary Table

Supplementary Table 1. Free amino acid composition of rabbit meat extract prepared under thermal extraction conditions (mg/100g)

Free amino acid	Content
o-phosphoserine	40.6
Taurine	263.4
o-phosphoethanolamine	16.1
L-Aspartic acid	95.8
L-Threonine	151
L-Serine	213.3
L-Glutamic acid	342.3
Sarcosine	20.1
Glycine	299.9

L-Alanine	352.7
L-Citrulline	2.7
L-Valine	178.5
L-Methionine	76.9
L-Cystathionine	5.3
L-Isoleucine	119.1
L-Leucine	277.2
L-Tyrosine	115.8
L-phenylalanine	131.4
β-Alanine	37.3
4-Aminobutyric acid	13.8
2-Aminoethanol	53.5
L-Ornithine	58.1
L-Lysine	205.7
L-1-Methylhistidine	10.7
L-Histidine	73.8
L-Anserine	1956.3
L-Carnosine	172.3
L-Arginine	57.4
L(-)-Proline	200.7